

Fusion excitation function revisited

Ph Eudes¹, Z Basrak², F Sébille¹, V de la Mota¹, G Royer¹ and M Zorić²

¹ SUBATECH, EMN-IN2P3/CNRS-Université de Nantes, P.O.Box 20722, F-44 307 Nantes, France

² Ruđer Bošković Institute, P.O.Box 180, HR-10 002 Zagreb, Croatia

E-mail: eudes@subatech.in2p3.fr

Abstract. We report on a comprehensive systematics of fusion-evaporation and/or fusion-fission cross sections for a very large variety of systems over an energy range $4A$ – $155A$ MeV. Scaled by the reaction cross sections, fusion cross sections do not show a universal behavior valid for all systems although a high degree of correlation is present when data are ordered by the system mass asymmetry. For the rather light and close to mass-symmetric systems the main characteristics of the complete and incomplete fusion excitation functions can be precisely determined. Despite an evident lack of data above $15A$ MeV for *all* heavy systems the available data suggests that geometrical effects could explain the persistence of incomplete fusion at incident energies as high as $155A$ MeV.

1. Introduction

Three regimes of fusion process only qualitatively explain the fusion excitation function [1]. The two low energy regimes have been thoroughly studied in the past as well as today [2]. On the contrary, the third high-energy regime related to the extinction of fusion cross section has been studied only occasionally. The question *how and why* the fusion process disappears did not receive a satisfactory answer yet. The two systematics on fusion excitation function data have been published so far, in 1984 by Mogenstern et al. [3] and by the Indra collaboration in 2006 [4] both being focused on rather light and symmetric systems. In the former study, the disappearance of complete fusion has been foreseen for $v_L < 0.19c$ and the onset of incomplete fusion for $0.06c < v_L$ ¹. For a symmetric system and in terms of incident energy these limits are respectively equal to $67A$ MeV and $6,7A$ MeV. In the present work we challenge both previously established limiting values. In the latter systematics, presented is a fusion excitation function for 7 light nearly symmetric systems. It has been found that quasi-fusion becomes vanishingly small above $50A$ MeV.

In this work we have considerably extended the previously published systematics and an exhaustive review of measured fusion cross sections available today at energies well above the Coulomb barrier ($E_{\text{LAB}} > 4A$ MeV) is presented. Undertaken a scrutiny scan of the published fusion data over the last forty years ended with 168 fusion cross section (FCS) values belonging to 57 different systems: A span in total system mass $A_{\text{tot}} = A_t + A_p$ (A_t and A_p stand for target and projectile mass, respectively) ranges between 26 and 246, system mass asymmetry

¹ v_L denotes the velocity of the lighter partner in the center-of-mass frame.

$\mu = |A_t - A_p| / (A_t + A_p)$ from 0 to 0.886, neutron to proton N/Z ratio from 1 to 1.536 while incident energy lies between $4A$ and $155A$ MeV.

Created high-energy excitation function for the fusion-evaporation and/or fusion-fission processes should allow 1) to pin down a possible regularity in the global available data set or in appropriately selected data subsets, 2) to identify a possible missing data and to establish a priority list of new measurements that would have to be performed and 3) to deliver a set of data that can be used to constrain microscopic transport models used to describe properties of heavy-ion collisions around the Fermi energy. In fact, reproducing the overall evolution as well as the main features (onset, maximum and extinction) of the global fusion excitation function or the one obtained by sorting data as a function of a given entrance channel parameter is a real challenge and a *sine qua non* condition for these models. Indeed, before pretending to describe in detail properties of the reaction exit channel such as creation and properties of particle species with their energy spectra and isospin these models firstly have to accurately reflect the global features of reaction mechanisms involved.

2. The raw data

In Fig. 1 are displayed all collected fusion data as a function of incident energy in the laboratory reference frame sorted by the increasing system mass A_{tot} . The systems are differentiated by a color code (online): blue and green symbols label the lighter systems ($26 < A_{\text{tot}} < 116$) while pink and red symbols the heavier ones ($146 < A_{\text{tot}} < 246$). Black symbols are used to point out measurements for which in the original publication is explicitly mentioned a possible overestimation of the fission component due to an unresolved contribution of fast-fission [5–8]. Black symbols are also used for the five systems labeled by *Only ER* in Fig. 1 for which the evaporation cross sections were measured only, whereas a more or less significant fission component was expected too [9, 10].

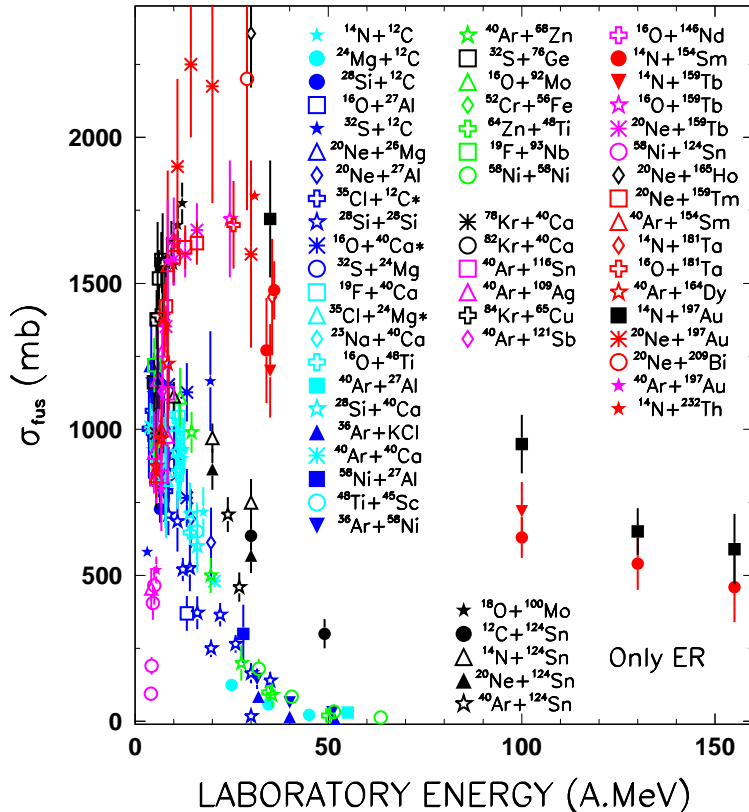


Figure 1. (Color online.) Raw fusion cross sections plotted as a function of the laboratory energy per nucleon E_{LAB}/A . The inventoried systems are distinguished among them by a color code which is used throughout this paper. For convenience, all the references are indicated in Figs. 3 and 4. See text for details.

It is instructive to investigate the systems by sorting them following both their mass asymmetry and their isospin. By a careful survey of the list of systems one infers easily that lighter systems (top of the list) are rather symmetric both in mass and isospin ($0 < \mu < 0.5$ and $1 < N/Z < 1.25$) while, on the contrary, heavier systems (bottom of the list) are very asymmetric in mass (for most of them $\mu > 0.75$) and, as expected, more asymmetric in isospin ($N/Z > 1.3$). The ensemble of fusion data splits into the two distinct sets exactly matching our color code. A first set corresponds to Light Symmetric Systems (LSS) for which FCS diminish with incident energy and disappear above 40–50A MeV (see also [4]). A second set corresponds to Heavy Asymmetric Systems (HAS) for which FCS increase up to 20A MeV and then decrease. The HAS branch surprisingly persists at energies as high as 155A MeV. At that point one must stress an evident lack of FCS data: For the heaviest systems in general data are scarce above 15A MeV, particularly for HAS between 30A and 100A MeV, and for systems of medium mass asymmetries in the entire energy range. Let us add that fusion data above 100A MeV are from a single experiment [8].

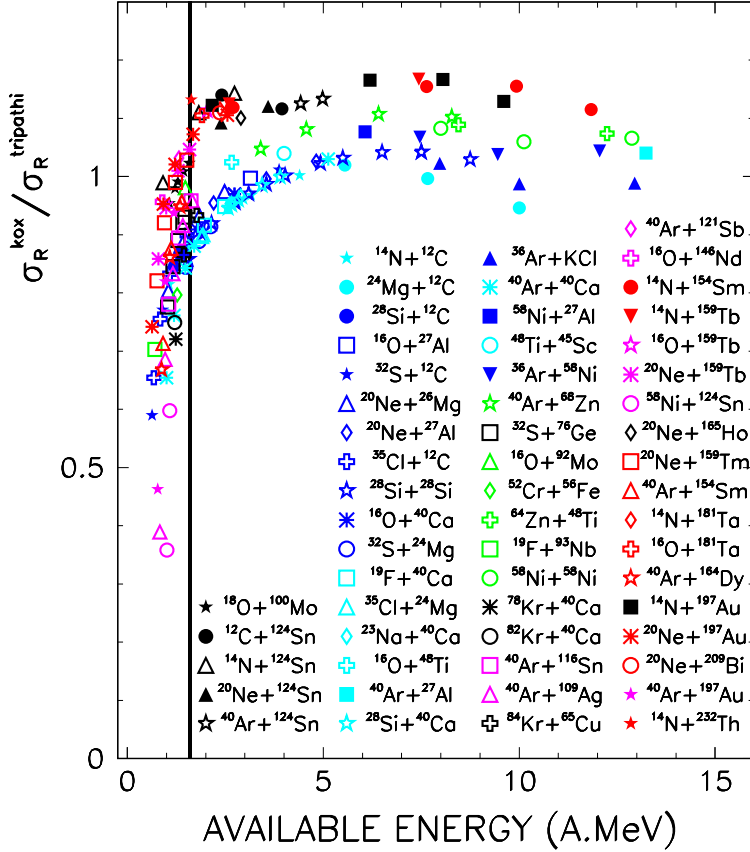


Figure 2. (Color online.) Kox over Tripathi reaction cross section $\sigma_R^{Kox} / \sigma_R^{Tripathi}$. The black vertical line indicates the $E_{c.m.}/A = 1.6A$ MeV limit. See text for details.

3. Normalization of the fusion cross sections

To reduce the effect of A_{tot} one normalizes FCS by reaction cross sections σ_{fus} / σ_R . By specifying abscissae in units of available energy (*i.e.* the system center-of-mass energy per nucleon $E_{c.m.}/A$) one expresses the mass asymmetric systems on the same footing with those which are mass symmetric. These coordinate scalings greatly ease the comparison of various systems with each other. Several parameterizations are used in calculation of reaction cross sections [11–16]. The parameterization of Tripathi is chosen because it is applicable for any combination of colliding nuclei and valid over the large energy range from a few A MeV to a few A GeV [11]. Note that

this parameterization depends on the root-mean-square charge radii of nuclei for which we used the tabulated values of Ref. [17]. Nevertheless, to check that our results do not depend too much on the chosen prescription, a comparison between the Kox [12] and Tripathi formulas has been performed, Kox formula being modified in order to extend its applicability down to a few A MeV similarly as Shen et al. have done [13]. The comparison is displayed in Fig. 2 where is shown the ratio $\sigma_R^{Kox}/\sigma_R^{Tripathi}$ of reaction cross sections calculated respectively by Kox and Tripathi formulas. Again, the two sets previously mentioned (LSS and HAS) are evident. For HAS, it is clear that this ratio is almost constant, varying between 1.09 and 1.17 for $E_{c.m.}/A > 1.6A$ MeV. Below this limit denoted by the thick vertical line in Fig. 2, the differences are growing and reach more than 60% at the lowest energies.

For LSS, the conclusion is similar except that the ratio is closer to 1 (within 10%). Subsequently, we will restrict the domain of validity of our analysis to $E_{c.m.}/A > 1.6A$ MeV where both formulas are quite compatible. Thus, choosing Tripathi formula as we have done, implies a slight difference in absolute values of normalized cross sections but does not alter the shape of the excitation function. Anyway, it is likely that none of these parameterizations is correct at such low energies. To recall this zone of inconsistency of evaluated total reaction cross sections σ_R in all next figures a yellow band is added for $E_{c.m.}/A < 1.6A$ MeV.

Figures 3 and 4 show the LSS and HAS data sets in the scaled coordinates, respectively. A particularly huge effect is observed for HAS, but clearly, contrary to what one may expect, FCS cannot be put under a universal behavior that would be valid for all systems. In fact, instead of following a single global law, plotted FCS strongly suggests the existence of two branches: a lighter symmetric one (Fig. 3) and a heavier asymmetric one (Fig. 4). These figures call for several comments. When only LSS are considered (Fig. 3), apart from a few points corresponding to the $N + C$ and $S + C$ systems, a very regular correlation is observed. The preliminary FCS data on a symmetric and rather heavy $Xe + Sn$ system reported at this Conference [62] seems to nicely fall in the mentioned systematics (not included in Fig. 3). The LSS excitation function can be very well reproduced by a hyperbolic function (see the solid red curve in Fig. 3).

The fit was achieved with the points located outside the yellow zone. The fit parameters, however, are quasi-independent on whether or not the points of the yellow zone are taken into account. The result is also independent on whether the Kox or Tripathi formula was used. Both σ_{fus} and σ_R depend on available energy. No obvious and simple physical explanation justifying the observed hyperbolic dependence can be drawn using *e.g.* $1/E_{c.m.}$ dependence as suggested in the Bass model [63]. It is probably due to a non-validity of this model at the highest energies of the so-called regime III of fusion process (see *e.g.* in Ref. [1]). Further important result is that incomplete fusion reaction mechanism clearly disappears around $E_{c.m.} = 12A$ MeV whatever the LSS system is. This findings is in agreement with the results of Ref. [4]. By using the microscopic transport Landau-Vlasov model [64] we have shown years ago that the fusion process abruptly disappears around the Fermi energy in head-on collisions: An elongated composite system gives rise to two nuclei of the reaction exit channel having kept a strong memory of the entrance channel suggesting a partial transparency phenomenon [65].

Understanding the HAS data subset seems to be less straightforward. Nevertheless, by neglecting the data points of the yellow zone and those labeled by *Only ER* the few remaining data suggest the existence of a second asymmetric branch of FCS tending towards a constant value at high incident energies. Can one explain the persistence of fusion at such high energies?

Above $100A$ MeV a crucial role that the reaction geometry plays in heavy ion collisions is a well established fact. In such geometrical picture, fusion can occur for collisions with an impact parameter smaller than b_{max} , a value corresponding to a complete overlap between the projectile and the target. Otherwise, for impact parameters greater than b_{max} , part of the projectile pursues its trajectory at small angle with a velocity close to the projectile one. Within this approximation and with a reaction in direct kinematics the fusion cross section is expressed

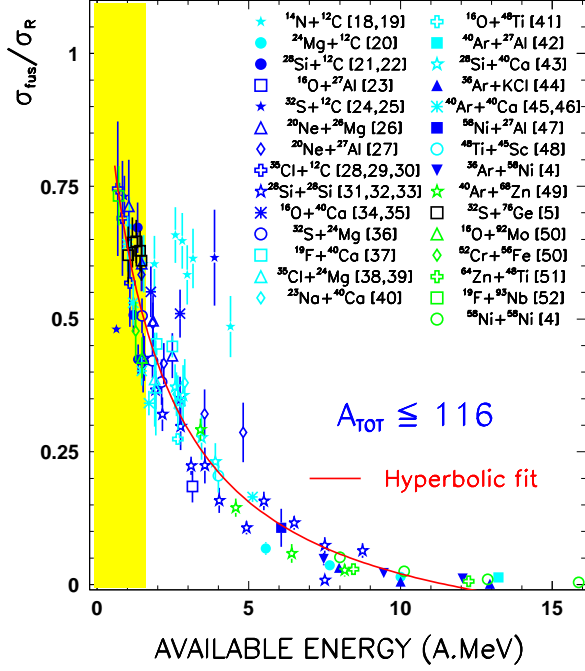


Figure 3. (Color online.) Normalized fusion cross sections for lighter and rather symmetric systems plotted as a function of $E_{\text{c.m.}}/A$. See text for details.

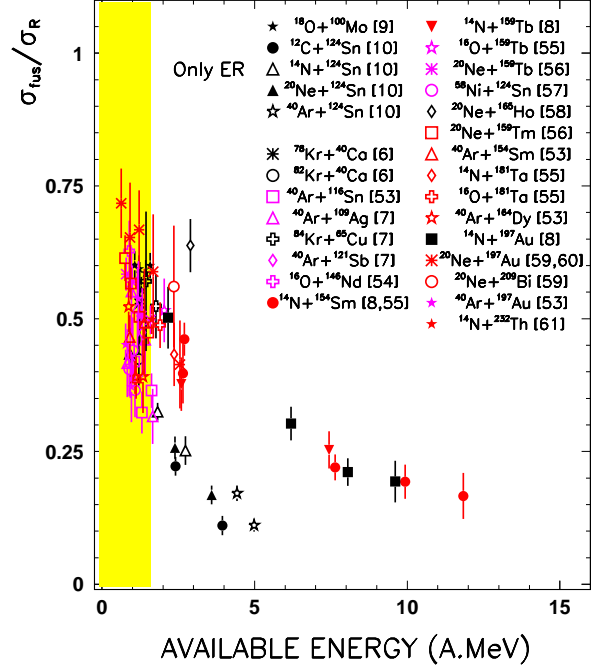


Figure 4. (Color online.) Same as Fig. 3 for heavier asymmetric systems. See text for details.

as following

$$\sigma_{\text{fus}} = \pi b_{\text{max}}^2 = \pi (R_t - R_p)^2 = \pi r_0^2 (A_t^{1/3} - A_p^{1/3}), \quad (1)$$

where R_p (R_t) is projectile (target) radius. Assuming the **simple** geometrical formula for the reaction cross section

$$\sigma_{\text{R}} = \pi r_0^2 (A_t^{1/3} + A_p^{1/3}), \quad (2)$$

one gets

$$\left[\frac{\sigma_{\text{fus}}}{\sigma_{\text{R}}} \right]_{\text{lim}} = \left[1 - \frac{2}{1 + (A_t/A_p)^{1/3}} \right]^2 = \left[1 - \frac{2}{1 + (\frac{1+\mu}{1-\mu})^{1/3}} \right]^2 \quad (3)$$

Eq. (3) indicates that at high energies normalized FCS tend towards a value which only depends on the mass asymmetry μ . For the $^{14}\text{N} + ^{154}\text{Sm}$ and $^{14}\text{N} + ^{197}\text{Au}$ Eq. (3) gives 14.4% and 17.0%, respectively in the very good agreement with experimental data. This reaction picture is confirmed by our Landau-Vlasov simulations [66]: For impact parameters of complete overlap collisions lead to the formation of a massive incomplete fusion nucleus accompanied by pre-equilibrium emission of light particles in the forward direction, an emission mostly originating from the projectile. Obviously, for a more and more symmetric system this limit tends to zero in accordance with what is observed experimentally. The mass asymmetry μ of the system seems to be the key parameter in explaining the above transition, at least in the high energy part. The data on systems of medium μ are needed to confirm or deny the above assumption.

4. Complete fusion excitation function

Among the experiments listed in our systematics only ten have explicitly been designed to measure both complete and incomplete fusion components [21, 25–27, 30, 31, 35, 36, 38, 43]. This

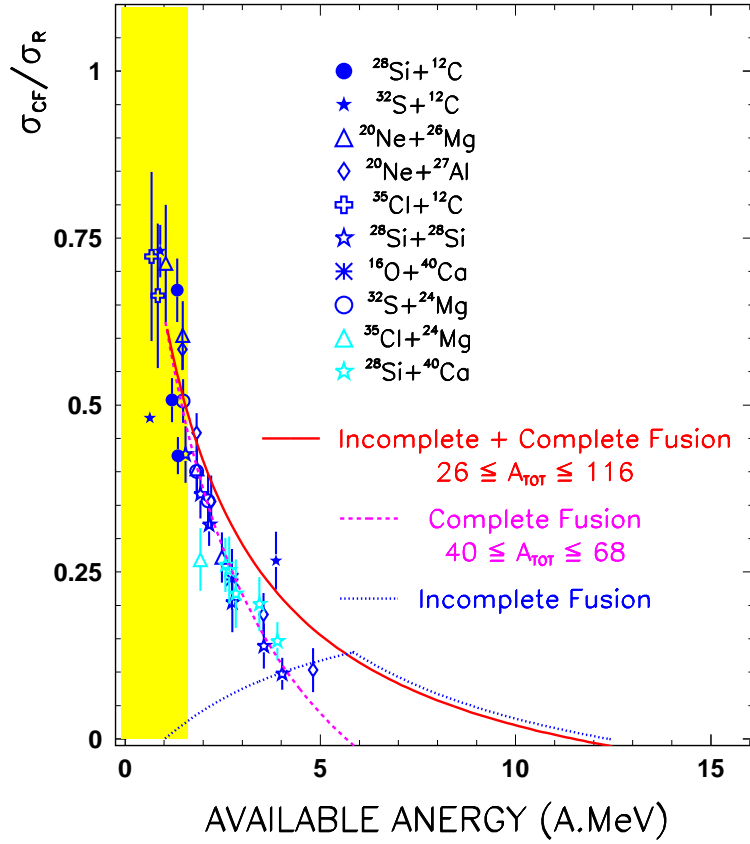


Figure 5. (Color online.) Normalized complete fusion cross sections for lighter symmetric systems plotted as a function of the available energy $E_{c.m.}/A$. See text for details.

allows establishing a complete fusion excitation function incorporating 29 FCS data points relative to 10 systems spanning a total mass range from 40 to 68. Data are reported in Fig. 5. Again, a very regular correlation is observed with FCS decreasing rapidly as a function of $E_{c.m.}/A$. As before, it can be fitted by the same kind of hyperbolic law (see pink solid curve in Fig. 5) which crosses abscissa around 6A MeV. For the complete fusion reaction mechanism, center-of-mass energy and excitation energy are equivalent. Thus, the energy limit of 6A MeV corresponds to the maximal excitation energy which can be deposited into a light compound nucleus. The above conclusion rises several questions. What happens for heavier systems? What for asymmetric systems? Does one obtain the same behavior and the same limit for complete fusion independently of A_{tot} ? Again, further measurements would be welcome.

Finally, in Fig. 5 are superimposed the two hyperbolic fits obtained for complete fusion (CF) and for the sum of CF and incomplete fusion (IF) components and which are denoted by pink and red curves, respectively as well as their difference which is colored blue. These functions provide a measure of the average contribution of CF and IF fusion components and of their evolution with energy. From the results of Fig. 5 one can, in particular, infer

- The threshold of IF is around $E_{c.m.}/A$ equal to 1A MeV.
- By increasing $E_{c.m.}/A$ CF decrease while IF increase. At 4A MeV each of these two components σ_{IF} and σ_{CF} contribute about the same value of $\approx 0.1 \times \sigma_R$ to the total reaction cross section.
- IF component increases up to 6A MeV where it reaches a maximum while at the same time the CF process vanishes. σ_{IF} reaches 15% of σ_R .
- After this maximum IF decreases and disappears around 12A MeV.

To our knowledge, it is the first time that such accurate limits concerning both CF and IF

fusion components are deduced from such a large body of data. It allows to draw a simple picture for the evolution of these reaction mechanisms.

5. Conclusions

In summary, we studied the energy dependence of fusion cross section aiming at understanding the evolution of the underlying reaction mechanisms as a function of entrance channel parameters and the causes of its (non-)disappearance. The heart of this work is a systematics and as wide as possible overview of measured fusion-evaporation and/or fusion-fission cross-sections including summed up complete and incomplete fusion contributions. Normalized by reaction cross sections and plotted as a function of the available energy per nucleon, the fusion cross sections show a rather universal behavior leading to a disappearance of the fusion around 12A MeV in the case of light symmetric systems. In the case of heavy asymmetric systems incomplete fusion seems to persist and tends towards a constant value depending only on the mass asymmetry of the system. In addition, dissociating available complete and incomplete fusion cross sections allows to provide fairly accurate energy limits characterizing these two mechanisms. Both the observed trends of fusion excitation function and the above limits place important constraints on the basic ingredients of microscopic transport models.

References

- [1] Bass R 1980 *Nuclear Reactions with Heavy Ions* (Berlin: Springer)
- [2] 2011 *EPJ Web of Conferences*, <http://www.epj-conferences.org> vol **17** *Proc. 5th Int. Conf. FUSION11 (Saint-Malo)*, ed. Schmitt C, Navin A, Rejmund M, Lacroix D and Goutte H (Berlin: Springer)
- [3] Morgenstern H *et al.* 1984 *Phys. Rev. Lett.* **84** 1104
- [4] Lauthesse P *et al.* 2006 *Eur. Phys. J.* **A27** 349
- [5] Guillaume G *et al.* 1982 *Phys. Rev. C* **26** 2458
- [6] Ademard G *et al.* 2011 *Phys. Rev. C* **83** 054619
- [7] Britt H C *et al.* 1976 *Phys. Rev. C* **13** 1483
- [8] Songzoni A A *et al.* 1996 *Phys. Rev. C* **53** 243
- [9] Kelly M P *et al.* 1997 *Phys. Rev. C* **56** 3201
- [10] Nifenecker H *et al.* 1985 *Nucl. Phys. A* **447** 533c
- [11] Tripathi A *et al.* 1997 *NASA Technical Paper* 3621
- [12] Kox S *et al.* 1987 *Phys. Rev. C* **35** 1678
- [13] Shen W *et al.* 1989 *Nucl. Phys. A* **491** 130
- [14] Sihver L *et al.* 1993 *Phys. Rev. C* **47** 1225
- [15] Shukla P *et al.* 2003 *Phys. Rev. C* **67** 054607
- [16] Abu-Ibrahim B 2011 *Phys. Rev. C* **83** 044615
- [17] Angeli I 2004 *At. Data and Nucl. Data tables* **87** 185
- [18] Stokstad R G *et al.* 1977 *Phys. Lett. B* **70** 43
- [19] Gomez del Campo J *et al.* *Phys. Rev. C* **19**, 2170 (1979)
- [20] Samri M *et al.* 2002 *Phys. Rev. C* **65** 061603R
- [21] Vineyard M F *et al.* 1993 *Phys. Rev. C* **47** 2374
- [22] Harmon B A *et al.* 1986 *Phys. Rev. C* **34** 552
- [23] Gilfoyle G P *et al.* 1992 *Phys. Rev. C* **46** 265
- [24] Giordano R *et al.* 1983 *Il Nuovo Cimento A* **77** 135
- [25] Kolata J J *et al.* 1985 *Phys. Rev. C* **32** 1080
- [26] Lehr H *et al.* 1984 *Nucl. Phys. A* **415** 149
- [27] Morgenstern H *et al.* 1983 *Z. Phys. A* **313** 39
- [28] Beck C *et al.* 1996 *Phys. Rev. C* **54** 277
- [29] Beck C *et al.* 1992 *Z. Phys. A* **343** 309
- [30] Pirrone S *et al.* 1997 *Phys. Rev. C* **55** 2482
- [31] Vineyard M F *et al.* 1990 *Phys. Rev. C* **41** 1005
- [32] Box P F *et al.* 1994 *Phys. Rev. C* **50** 934
- [33] Meyer R J *et al.* 1991 *Phys. Rev. C* **44** 2625
- [34] Vigdor S E *et al.* 1979 *Phys. Rev. C* **20** 146
- [35] Beck C *et al.* 1989 *Phys. Rev. C* **39** 2202
- [36] Hinnefeld J D *et al.* 1987 *Phys. Rev. C* **36** 989

- [37] Rosner G *et al.* 1985 *Phys. Lett. B* **150** 87
- [38] Cavallaro S *et al.* 1998 *Phys. Rev. C* **57** 731
- [39] Beck C *et al.* 1998 *Eur. Phys. J. A* **2** 281
- [40] Pochodzalla J *et al.* 1986 *Phys. Lett. B* **181** 33
- [41] Gonthier P L *et al.* 1983 *Nucl. Phys. A* **411** 289
- [42] Péter J *et al.* 1995 *Nucl. Phys. A* **593** 95
- [43] Vineyard M F *et al.* 1992 *Phys. Rev. C* **45** 1784
- [44] Bisquer E 1996 *Caractérisation de la fusion incomplète dans les réactions Ar+KCl 32, 40, 52 et 74 MeV/u*
Ph.D.Thesis, Université Claude Bernard (Lyon, France: Université Lyon I)
- [45] Rosch W *et al.* 1987 *Phys. Lett. B* **197** 19
- [46] Carter J *et al.* 1983 *Z. Phys. A* **313** 57
- [47] Lebreton L *et al.* 1998 *Eur. Phys. J. A* **3** 325
- [48] Stege H *et al.* 1988 *Nucl. Phys. A* **489** 146
- [49] Fahli A *et al.* 1986 *Phys. Rev. C* **34** 161
- [50] Agarwal S *et al.* 1980 *Z. Phys. A* **296** 287
- [51] Steckmeyer JC *et al.* 1996 *Phys. Rev. Lett.* **76** 4895
- [52] Tomar B S *et al.* 1998 *Phys. Rev. C* **58** 3478
- [53] Logan D *et al.* 1980 *Phys. Rev. C* **22** 1080
- [54] Oeschler H *et al.* 1983 *Phys. Lett. B* **127** 177
- [55] Prindle D *et al.* 1998 *Phys. Rev. C* **57** 1305
- [56] Cabrera J *et al.* 2003 *Phys. Rev. C* **68** 034613
- [57] Wolfs F L H *et al.* 1987 *Phys. Lett. B* **196** 113
- [58] Hilscher D *et al.* 1987 *Phys. Rev. C* **36** 208
- [59] La Rana G *et al.* 1983 *Nucl. Phys. A* **407** 233
- [60] Egelhaaf C *et al.* 1983 *Nucl. Phys. A* **405** 397
- [61] Leegte H K W *et al.* 1992 *Phys. Rev. C* **46** 991
- [62] Chbihi A *et al.* 2012 *J. Phys.: Conf. Series* this issue
- [63] Bass R 1974 *Nucl. Phys. A* **231** 45
- [64] Remaud B, Sébille F, Grégoire C, Vinet L and Raffray Y 1985 *Nucl. Phys. A* **447** 555c
Sébille F, Royer G, Grégoire C, Remaud B and Schuck P 1989 *Nucl. Phys. A* **501** 137
- [65] Basrak Z and Eudes Ph 1999 *Proc. 7th Int. Conf. on Clustering Aspects of Nuclear Structure and Dynamics (Rab, Croatia)* ed. Korolija M, Basrak Z and Čaplar R (Singapore: World Scientific) p. 316
- [66] Eudes Ph *et al.* Work in preparation for publishing